Nanodielectrophoresis: Electronic Nanotweezers

P. J. Burke

Department of Electrical and Computer Engineering, University of California, Irvine, California, USA

CONTENTS

1. INTRODUCTION

At neutral pH, DNA is a charged molecule. As such, it responds directly to an electric field, the phenomenon of *electrophoresis*. In contrast, the phenomenon of *dielectrophoresis* occurs when there is a dc or an ac electric field *gradient*. In that case, the development of nonuniform electric fields causes a force on any polarizable object, charged or neutral. The term dielectrophoresis was coined by Pohl in 1951 [1], and the general principles are outlined in his 1978 book of the same title [2]. Since then, the use of microfabricated electrodes has been employed for separating micron-sized objects such as cells, and this technology is currently being integrated with lab-on-a-chip systems. This review article discusses recent progress at extending the practice of dielectrophoresis to the nanoscale, for applications in nanomanufacturing, nanobiotechnology, and molecular electronics. Compared to the use of dielectrophoresis for the manipulation of cells, the use of electric fields at the nanoscale to assemble nanocircuits is still in its infancy.

1.1. Other Reviews

The main reference for the fundamentals of dielectrophoresis is Pohl's 1978 book [2]. The physics of the dielectric properties of biological molecules in solution are covered in a 1979 book by Pethig [3] and a 1978 book by Grant et al. [4]. Pethig [5, 6] has a good review of applications of dielectrophoresis in biotechnology. Another review article covering the manipulation of cells with electric fields is in Führ's 1996 book chapter [7, 8]. The topic of dielectrophoresis is covered in Madou's textbook on microfabrication [9]. A review by Hughes [10] discusses some applications of dielectrophoresis in nanotechnology. This review will also be concerned primarily with the applications of dielectrophoresis in nanotechnology. Nanodielectrophoresis.

2. OVERVIEW OF DIELECTROPHORESIS

The discovery of dielectrophoresis (DEP) goes all the way back to at least 600 B.C., when Thales of Miletus in Turkey observed that rubbed amber attracted small particles of fluff [2]. In retrospect the amber, being charged up from the rubbing, generated an electric field which polarized the fluff particles. The induced dipole in the fluff particles was acted on by the (nonuniform) electric fields, attracting it to the charged amber. Today we would call this effect (dc) positive dielectrophoresis.

In Figure 1, the principle is illustrated schematically. If a polarizable object is placed in an electric field, there will be an induced positive charge on one side of the object and an induced negative charge (of the same magnitude as the induced positive charge) on the other side of the object. The positive charge will experience a pulling force; the negative charge will experience a pushing force. In a uniform field, as depicted in Figure 1A, the pulling force will cancel the pushing force, and the net force will be zero. However, in a nonuniform field, as depicted in Figure 1B, the electric field will be stronger on one side of the object and weaker on the other side of the object. Hence, the pulling and pushing

ISBN: 1-58883-001-2/$35.00

Encyclopedia of Nanoscience and Nanotechnology
Edited by H. S. Nalwa
Volume X: Pages (1–19)

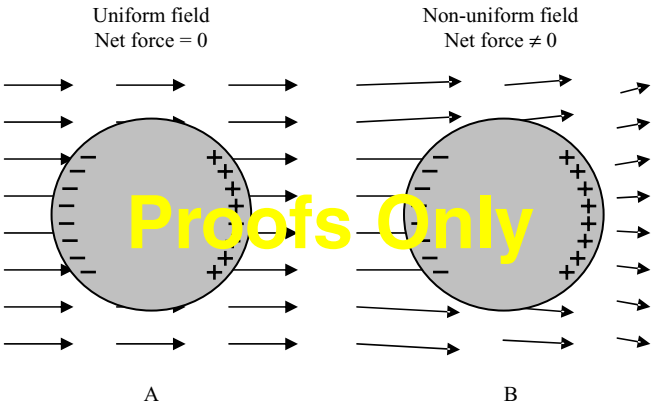

Figure 1. Schematic depiction of dielectrophoresis. The direction of the arrows represents the direction of the electric field; the length of the arrows represents the magnitude of the electric field.

forces will not cancel, and there will be a net force on the object.

In this simple overview we have neglected the polarizability of the surrounding medium. If both the medium and the polarizable particle are considered, then one comes to the conclusion that there are two classes of DEP: positive and negative. If the suspended particle has a polarizability higher than that of the surrounding medium, then the DEP force pushes the particle toward the higher electric field region. This is called *positive dielectrophoresis*. If the suspended particle has a polarizability less than the surrounding medium, the particle is pushed toward the region of weaker electric field, and this is called *negative dielectrophoresis*.

2.1. Quantitative Force Predictions

In an electric field $\vec{E}$, a dielectric particle behaves as an effective dipole with (induced) dipole moment $\vec{p}$ proportional to the electric field, that is,

$$\vec{p} \propto \vec{E} \tag{1}$$

The constant of proportionality depends in general on the geometry of the dielectric particle. In the presence of an electric field gradient, the force on a dipole is given by

$$\vec{F} = (\vec{p} \cdot \vec{\nabla})\vec{E} \tag{2}$$

Combining the two equations, and using known results for the relationship between $\vec{p}$ and $\vec{E}$ for a *spherical* particle of radius r and dielectric constant ϵ_p, and taking into account the medium dielectric constant ϵ_m, it can be shown that the force acting on a spherical particle (the *dielectrophoresis* force) is given by [2, 11]

$$\vec{F}_{DEP} = 2\pi v \epsilon_m \alpha_r \vec{\nabla}(\vec{E}^2_{RMS}) \tag{3}$$

where v is the volume of the particle, $\vec{E}_{RMS}$ is the RMS value of the electric field (assuming a sinusoidal time dependence), and α_r is the real part of what is called the *Clausius–Mosotti* factor, which is related to the particle dielectric constant ϵ_p and medium dielectric constant ϵ_m by

$$\alpha_r \equiv Re\left(\frac{\epsilon_p^* - \epsilon_m^*}{\epsilon_p^* + 2\epsilon_m^*}\right) \tag{4}$$

Here the star (*) denotes that the dielectric constant is a complex quantity, and it can be related to the conductivity σ and the angular frequency ω through the standard formula

$$\epsilon^* = \epsilon - i\frac{\sigma}{\omega} \tag{5}$$

Equation (5) also takes into account surface conductances [12–14] of the particles.

We must make several comments now about Eq. (3). First of all, the Clausius–Mosotti factor can vary between -0.5 and $+1.0$. When it is positive, particles move toward higher electric field regions, and this is termed *positive dielectrophoresis*. When it is negative, the particles move toward smaller electric field regions, and this is termed *negative dielectrophoresis*.

Second, the force grows smaller as the particle volume. This has important implications for the manipulation of nano-sized particles, as we will discuss below. Of course this is a bulk, classical calculation. Surface charges and quantum effects will no doubt be important at the molecular level, and these need to be dealt with. Therefore, the application of Eq. (3) to single molecules may not be quantitatively valid.

Third, the dielectric constants of the medium and particle can be highly frequency dependent. This gives rise to a force that can be different at different frequencies, and this fact can be exploited for practical micro- and nanomanipulations based on dielectrophoresis. For example, at one frequency positive dielectrophoresis may prevail, while at another frequency negative dielectrophoresis may prevail. These effects are all buried in the physics of the dielectric response function ϵ.

Fourth, the derivation of Eq. (3) assumes that the electric field does not vary too strongly; this will have implications when we compare to optical tweezers below.

Finally, Eq. (3) is true for both dc *and* ac electric fields. While there are practical advantages to using ac electric fields to be discussed below, the mathematics of the dielectrophoresis force does not differentiate between dc and ac. Furthermore, it should be noted that the *direction* of the electric field does not matter. That is to say, in the dc case, for (e.g.) positive dielectrophoresis, the particle moves from the region of weaker field to the region of stronger field *magnitude*, regardless of the *direction* in which the field is pointing. For an ac field, the particle experiences a time-varying force, but the time-averaged direction of that time-varying force is always the same, even though the direction of the electric field vector is changing in time. In most cases, the ac component of the dielectrophoretic force can be neglected and we need only concern ourselves with the dc (i.e., time-averaged) component, which is the one given by Eq. (3).

2.2. Generation of Electric Field Gradients

Historically [2], the use and study of dielectrophoresis was between a sharp pin and a flat surface, because that is the easiest geometry in which one can create a strong field gradient, hence a strong dielectrophoretic force. This has been used to manipulate cells in solution [5, 6], since a cell is polarizable. It has also been used to deflect individual molecules in molecular beams [15]. This application can be considered the first application of nanodielectrophoresis, although the molecular beams were in a high-vacuum system.

Since the advent of optical and then electron-beam lithography, the use of micro- and nanofabricated planar metal electrodes on insulating substrates has achieved much more attention, since it allows many different flexible geometries to be designed, tested, and used. Moreover, by using small gaps between electrodes, large electric field strengths can be achieved, thus further increasing (in general) the achievable dielectrophoretic force.

Although any arbitrary geometry for planar electrodes can be easily designed and fabricated with modern lithography, the three most commonly used geometries are shown in Figure 2. (The DEP force from these and other geometries can be calculated numerically [16, 17].) Part A shows the simplest geometry, a gap between two electrodes. Because the electrodes are planar, there will be fringing fields out of the plane which are very nonuniform. This design is useful for positive dielectrophoresis, in which case particles are attracted to the edges of the electrodes, or negative dielectrophoresis, in which case particles are pushed away from the plane of the electrodes. In order to achieve a higher electric field gradient, geometry B is sometimes used. The castellations can be square (as shown), triangular, or circular. For both geometries A and B, interdigitated fingers are often used. Geometry C is used normally for negative dielectrophoresis. Huang and Pethig showed that particles experiencing negative dielectrophoresis that are in the plane of the electrodes will get trapped in the center of the electrode geometry [18]. Another design which has received some attention is a spiral electrode design [19].

Modern interest in nanodielectrophoresis, in contrast to that applied to molecular beams in high-vacuum environments, is concerned with the manipulation of molecules in solution, especially for applications in nanobiotechnology, where wet environments are necessary for life itself, but also as methods of nanomanufacturing molecular electronic circuits, integrated with micro- and nanofabricated electrodes. After the dielectrophoresis-assisted nanofabrication occurs, the sample can be dried and the remaining molecules that were placed in position while dissolved now can form the basis of some tailor-designed circuit which in principle was fabricated one molecule at a time. This vision is currently under development but in principle there is no reason it cannot be achieved, as we discuss in the remainder of this article.

2.3. Traps for Negative Dielectrophoresis

For negative dielectrophoresis, the polarizable objects feel a force pushing them *away* from the high field region. Therefore, for most planar geometries, the particles are pushed away from the substrate where the electrodes reside. In 1991, Huang and Pethig calculated [18] the necessary geometry that electrodes need to have in order to *trap* particles using negative dielectrophoresis at specific locations on the plane of the substrate. The geometry they found which traps a particle at a specific point in the plane of the electrodes is a quadrupole-like geometry. This trap is only in two dimensions, and in the third dimension (perpendicular to the plane of the electrodes), the particle is still not trapped. Gravity or some other force must be exerted to bring the particle close enough to the plane of the electrodes to feel the dielectrophoretic force of the electrodes.

Later, work of Schnelle and co-workers [20] and Fuhr and co-workers [21] considered geometries necessary for trapping of particles in all three dimensions. They name these traps "cages." The most straightforward geometry realized and tested consisted of two quadrupole traps fabricated on two microscope slides which were mounted facing each other with a small gap (of about 0.1 mm). In that work, they trapped 10-μm latex particles and cells in three dimensions, with applied ac voltages up to 1 GHz in frequency.

We show in Figure 3 an example realization of a quadrupole trap: four gold electrodes surrounding a central

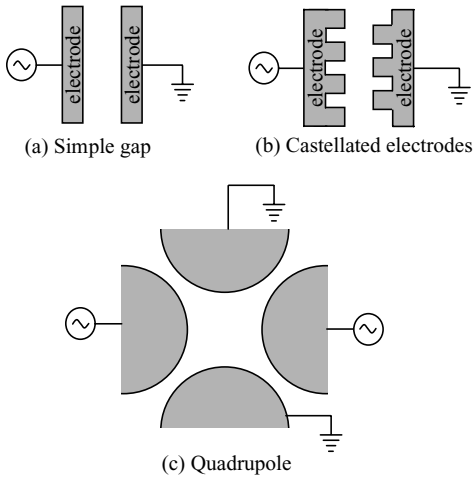

Figure 2. The most commonly used geometries for the study of dielectrophoresis. The electrodes are usually thin metal films (1–100 nm) fabricated lithographically on an insulating substrate.

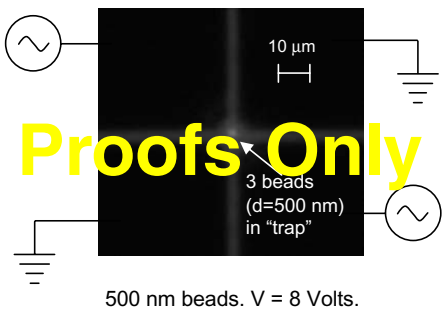

Figure 3. Electrodes to trap small particles. Three 500-nm beads can be seen fluorescing but not resolved. We have also been able to trap a single 500-nm bead (not shown).

region with 10-μm gaps are used to trap a 500-nm latex bead [22]. The frequency used for these studies was 1 MHz, with a voltage of 8 V. With smaller gaps it should be possible to trap much smaller particles, as we discuss below.

2.4. Scaling with Particle and Electrode Size

In order to calculate the force acting on any given polarizable particle, one can use Eq. (3) as long as the electric field intensity and (more importantly) its spatial gradient are known. For arbitrary electrode geometries it is possible to numerically calculate this force. However, some simple electrode geometries can be calculated analytically in order to give some general insight into what can be expected for a more complicated geometry. The case of two concentric spheres in this regard can be very enlightening, as the radius of curvature can be used as a rough estimate for the smallest feature size of a given electrode.

The electric field between two concentric spheres is straightforward to calculate, and based on this one can calculate the gradient of the electric field intensity. One finds [2]

$$\vec{\nabla}(\vec{E}_{RMS}^2) = -\frac{2r_1^2 r_2^2 V^2}{r^5(r_2 - r_1)^2}\hat{r} \tag{6}$$

where $\hat{r}$ is a unit vector in the radial direction, r_1 is the radius of the inner electrode, r_2 is the radius of the outer electrode, r is the distance from the origin, and V is the applied voltage, as shown in Figure 4. In the case where the inner electrode is very sharp compared to the distance to the outer electrode (i.e., $r_1/r_2 \ll 1$), this becomes

$$\vec{\nabla}(\vec{E}_{RMS}^2) \approx -\frac{2r_1^2 V^2}{r^5}\hat{r} \tag{7}$$

In this case the force exerted on a particle is given by

$$\vec{F}_{DEP} = -4\pi v \epsilon_m \alpha_r \frac{r_1^2 V^2}{r^5}\hat{r} \tag{8}$$

Now, if the particle were in a vacuum with no other forces acting upon it, then it would respond only to the DEP force. However, in solution, the particle is undergoing Brownian motion, and is continually being bombarded with other molecules of the solution. This thermal motion exerts

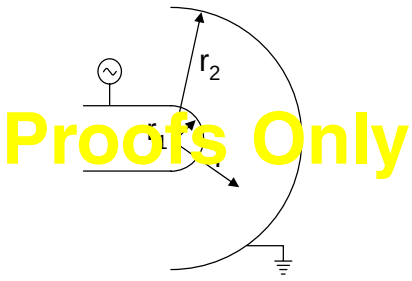

Figure 4. Spherical geometry electrodes for analytical calculation of dielectrophoretic force in the text.

an effective random force on the particle, whose maximum value is given roughly by [2]

$$F_{thermal} \approx k_B T/2r_{particle} \tag{9}$$

where k_B is the Boltzmann constant, T is the temperature, and $r_{particle}$ is the particle radius.

For DEP to be of use, the DEP force must overcome the randomizing thermal motion acting on the particle. In 1978, Pohl used 500 μm for the radius of the inner electrode, 5000 V for the applied voltage, and 1 mm for the particle distance from the electrode, and concluded that particles smaller than 500 nm would not respond very well to the DEP force [2]. These numbers were pessimistic, and it should be possible to trap 1-nm and smaller particles, as we now show.

First, as our experiments [22], as well as other experiments [23–31] show, it is possible to use optical or electron-beam lithography to fabricate electrodes with much smaller radius of curvature than 500 μm (as Pohl originally assumed), and hence to trap submicron particles (see Fig. 3). For example, in our experiments, we trapped 500-nm beads with less than 10 V applied to the electrodes.

Second, it is possible in principle to use carbon nanotubes or other nanowires as the electrodes themselves [22], which would have radius of curvatures of less than 1 nm. In this case, for a 1-nm particle that was a distance 100 nm away from the nanotube electrode, our calculations [32] indicate that the DEP force would exceed the thermal force at an applied voltage of only 50 mV. Experiments to test this scaling prediction with carbon nanotube electrodes are currently underway in the author's lab [22].

2.5. Electrorotation

Another effect of an ac electric field on a polarizable object is to *orient* that object with respect to an electric field. Specifically, the induced dipole moment of an object interacts with the electric field to produce a torque given by

$$\vec{T} = \vec{p} \times \vec{E} \tag{10}$$

where $\vec{p}$ is the induced dipole. This effect can be used to orient DNA and nanotubes in solution, and also nanotubes during growth in gas or vacuum, as we will discuss below. It also can be used to orient cells and other micron-sized objects. The term *electrorotation* is usually applied to a situation where the direction of the electric field is rotating as a function of time. This can be achieved by using four electrodes surrounding a central region, where the ac voltage on each electrode is properly phased. Under the rotating electric field direction, the torque also rotates, and hence the particle rotates. This effect is reviewed in [8, 33].

2.6. Traveling Wave Dielectrophoresis

The electrode geometries shown in Figure 2 are useful for trapping particles with either positive or negative dielectrophoresis. However, more sophisticated geometries are possible that allow a particle to be moved. Figure 5 shows schematically a set of electrodes with ac voltages adjusted in such a way as to generate a traveling wave electric field. This traveling wave can act on a polarizable particle and cause

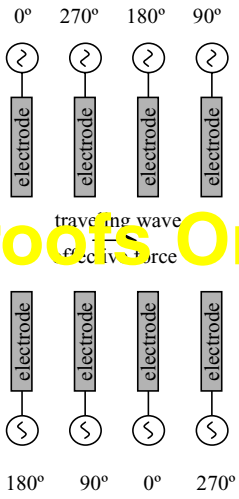

Figure 5. Schematic electrode geometry for traveling wave dielectrophoresis.

a net force in the direction of the traveling wave. In [34], Hagedorn et al. analyze geometries optimum for traveling wave dielectrophoresis. Fuhr in 1994 was able to design and demonstrate a particle manipulator that could apply force in two orthogonal directions [35].

2.7. Summary

The combined effects of dielectrophoresis, electrorotation, and traveling wave dielectrophoresis (TWD) have all gone under the same name: "pondermotive force," as they have the same underlying physical origin. The relationship among these effects is explored in more detail in [8, 36–40]. With the combined use of dielectrophoretic traps, traveling wave dielectrophoresis, and electrorotation, it is possible to electronically control (via microfabricated electrodes) the three-dimensional position and orientation of a small micro- or nanoparticle that is suspended in liquid.

3. ELECTRONIC VERSUS OPTICAL TWEEZERS

From Eq. (3), we calculate that a typical dielectrophoretic force for a particle of size 100 nm will be roughly 1 fN; the force on a 1-μm particle would be roughly 1 pN. In comparison, the force exerted by optical tweezers [41–46] is also the same order of magnitude. In fact both optical tweezers and dielectrophoresis are the same physical phenomena, only different frequencies. For example, our Eq. (3) is equivalent to Eq. (2) in [44]. (There is a factor of $4\pi\epsilon_m$ difference due to the units, and an incorrect sign in the denominator of [44].) The equations look a little bit different, because optical engineers like to use the index of refraction, and electrical engineers like to use the dielectric constant; they are of course related through $n = \sqrt{\epsilon}$.

A difference between optical tweezers and electronic tweezers is that optical tweezers also affect particles whose size is comparable to the (optical) wavelength, of order μm, the so-called Mie limit. The analogy with electronic tweezers is more appropriate in the limit where the particle size is smaller than the optical wavelength λ, the so-called Rayleigh limit. For optical tweezers in the Rayleigh limit (particle size $\ll \lambda$), the force is proportional to the volume of the particle, as in DEP Eq. (3). For optical tweezers in the Mie limit (particle size $\gg \lambda$), the force is independent of the particle size. Furthermore, optical scattering of light in optical tweezers is an important force, whose analog in electronic tweezers is not clear-cut.

One main similarity between optical and electronic tweezers is that, when applied to particles in solution, both must strive to overcome the random forces due to Brownian motion. Hence, it makes sense that the induced forces for both optical and electronic tweezers exert comparable forces. To date, both electronic and optical tweezers have not trapped particles with size below 10 nm. However, with nanowire or nanotube electrodes we predict that electronic tweezers can trap particles down to 1 nm in size, which may be useful for nanoassembly.

An advantage that electronic tweezers have over optical tweezers is *scalability*: millions or even billions of electronic tweezers could be easily, economically integrated onto a silicon chip for low-cost "lab-on-a-chip" systems. Additionally, the electronic trap can in principle hold a particle indefinitely, while the optical tweezers in some cases only last for a few seconds due to laser-induced damage. Third, the use of optical tweezers is not possible in optically opaque systems; in contrast, the use of electronic tweezers is difficult in conducting solutions [47], a severe restriction for *in vivo* operation.

Thus, as with everything, both types of tweezers have their own advantages and disadvantages; the choice of which to use will depend upon the application. In fact, in some applications, both types of tweezers have been used in the same experiment [48].

4. TRAPPING AND MANIPULATION OF MICRON-SIZED OBJECTS

4.1. Steel Balls

In a pioneering patent [49] granted in 1983, Batchelder proposed the use of lithographically patterned microelectrodes to manipulate and position chemical species, potentially with the ability to manipulate a single molecule, for electronic control of manufacturing. As such, this patent covers the lab-on-a-chip concepts as well as single molecule dielectrophoresis very well, much ahead of its time. Batchelder further described his techniques in a 1983 article [50], where he described one of the first instances of "traveling wave dielectrophoresis." That was also one of the first instances of photolithographically patterned electrodes for applications in dielectrophoresis. Batchelder's realization experimental apparatus was capable of manipulating 600-μm steel balls and 1-mm water droplets in heptane.

In 1987, Washizu and co-workers used this effect to manipulate 15-μm solid particles in solution, and also proposed to use it for moving cells [51]. A year later they reported moving blood cells (sheep erythrocytes) using this effect [52]. Those initial experiments were on traditionally machined electrodes.

4.2. Cells

Interestingly, in two papers appearing in 1989 and 1990 [53, 54], Masuda and co-workers used photolithography for fabricating microelectrodes in order to use DEP to control the position of living cells. They also developed what they coined "fluidic integrated circuit," which currently would go by the term "lab-on-a-chip." They used photolithography and a molding process with silicone to make microfluidic channels capable of handling individual cells, and they made a cell-sorter based on dielectrophoresis: cells entering through one microfabricated inlet could be deflected electronically into one of two microfabricated outlets. We show in Figure 6 an example of using negative dielectrophoresis to trap human breast cancer cells in a planar quadrupole trap [55].

As this review is meant to cover mainly nanodielectrophoresis, we will only briefly highlight some of the applications of dielectrophoresis in cell manipulation. The polarizability of a cell is a complicated function of its membranes and inner workings generally, and generally depends on frequency. By exploiting the difference in the frequency-dependent dielectric properties of different cells, it is possible to separate out many different kinds of cells from one another and from other microorganisms in solution.

The first separation of viable and nonviable (yeast) cells by dielectrophoresis was in 1966 [56]. Chloroplasts were manipulated in 1971 [57]. Cells can undergo both positive and negative dielectrophoresis as was shown in [58, 59]. The separation of viable versus nonviable yeast cells was studied carefully with microfabricated electrodes in [60–62]. Different species of bacteria were separated in [63, 64]. Electrorotation was used to separate leukemia cells from blood in [65]. Electrorotation was used to separate human breast cancer cells from blood in [66]. Concentration of CD34+ from peripheral-stem-cell harvests was achieved in [67].

TWD linear motion of cells was shown in [34, 68]. Viable and nonviable yeast cells were separated with TWD in [69]. TWD was used to separate white blood cells from erythrocytes in [70]. Continuous separation is also possible (viable vs. nonviable yeast cells) [71]. Separation of trophoblast cells from peripheral blood mononuclear cells was achieved in [72]. Separation of breast cancer cells from normal T-lymphocytes (among other things) was achieved using DEP FFF (see next section) in [73]. The manipulation of E. coli and other bacteria with photolithography-fabricated electrodes was reported in 1988 in [74]. The E. coli were attracted to the high fringing field regions of interdigitated castellated electrodes. Cervical carcinoma cells were separated from peripheral blood cells in [75]. Living (Eremosphaera Viridis) cells were trapped in quadrupole and octopole traps in [20]. An extruded-quadrupole geometry (where the electrodes are metallic posts) was used for cell manipulation in [76]. The effect on cells of the large electric field strengths necessary for DEP (typically 10^6 V/m) was investigated by Archer et al. [77], who found a 20–30% increase in the expression of fos protein, as well as up-regulation of unidentified genes. While the large electric fields are not fatal to cells studied, and their long-term effect on cells manipulated with DEP seems to be minimal, at this stage there is insufficient evidence to draw more quantitative conclusions about the effects of exposure to high electric fields.

We note that, once the electrodes are in place for the dielectrophoretic manipulation of cells, it is straightforward and economical to integrate further optical and electronic measurements that are complementary to DEP techniques into the same measurement platform. These can include optical and electronic methods of genetic expression profiling using microarrays, with applications in point-of-care clinical diagnostics, biological warfare detection, and many other applications. For example, Cheng and co-workers separated E. coli bacteria from a mixture containing human blood cells and integrated this with cell lysing and DNA hybridization analysis on a single chip [78]. The integration of electrophoresis and dielectrophoresis using the same electrodes for manipulating E. coli cells with DEP and antibodies with electrophoresis was developed in [79]. DEP was used to separate certain cell types from complex cell populations, which significantly improved the accuracy of gene expression profiling in [80]. In the spirit of integration mentioned above, an integrated system using DEP, DNA amplification, and electronic DNA hybridization for the detection of E. coli and other biological agents was recently developed [81].

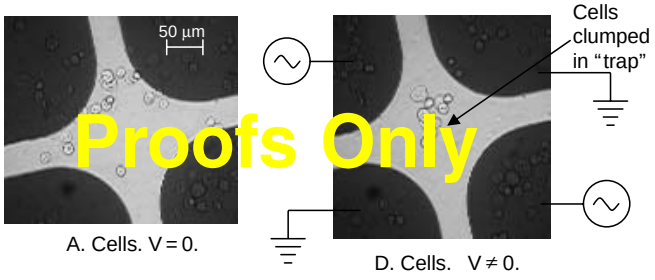

Figure 6. Dielectrophoretic trapping of human breast cancer cells (cell line HCC1806 from ATCC).

4.3. Field Flow Fractionation (FFF)

Field flow fractionation (FFF) is a very general chromatographic separation technique in chemistry and biology [82]. The use of dielectrophoresis as the force in field flow fractionation was proposed and analyzed by Davis and Giddings in 1986 [83]. The principle of dielectrophoretic field flow fractionation (DEP FFF) is shown schematically in Figure 7. Part A shows interdigitated finger electrodes, and parts B and C depict the levitation of latex beads when an ac voltage is applied to the electrodes. The levitation height is a function of the dielectric properties of the particle being levitated. If these electrodes are introduced into a laminar flow chamber (typically 100 μm thick), the flow velocity parallel to the chamber walls is also a function of height, as indicated schematically in part D. Thus, the speed at which a particle is swept through the chamber depends on the height at which it is levitated, which in turn is a function of its dielectric properties. Since different types of particles (or cells) generally have different dielectric properties, each takes a different time to traverse the chamber. This dependence can be used to separate different particles or cells, and is termed dielectrophoretic field flow fractionation (DEP FFF).

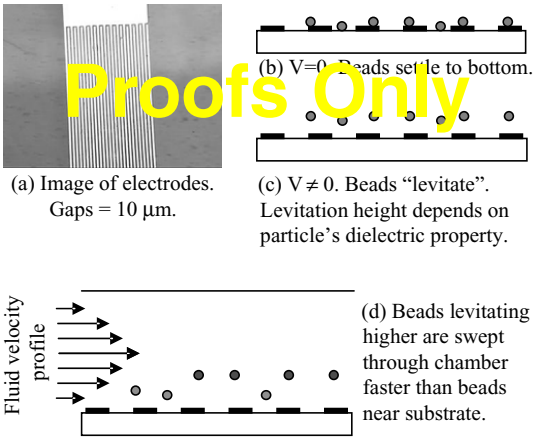

Figure 7. Schematic depiction of dielectrophoretic field flow fractionation (DEP FFF).

In 1994, Washizu and co-workers constructed a DEP FFF apparatus and used it to trap DNA of various sizes (9–48 kbp) and the protein avidin [84]. They were able to trap each macromolecule with some efficiency, but separation experiments were not reported. Initial experimental demonstration of DEP FFF separation was reported in 1997, where viable and nonviable yeast cells were separated [85], and human leukemia cells were separated from peripheral blood mononuclear cells [86]. In the same year, demonstration experiments on latex beads were performed [87]. Later experiments have demonstrated the separation of erythrocytes from latex beads [88], separation of mixtures of polystyrene beads [89], and the separation of human breast cancer cells from CD34+ stem cells [73, 90].

Thus, DEP FFF has been successfully demonstrated as a viable technique to separate many micron-sized objects such as cells and latex beads. However, the principles should also be applicable at the nanoscale, and it should in principle be possible to separate objects such as DNA, proteins, viruses, nanoparticles, nanowires, nanotubes, quantum dots, and possibly even small molecules.

5. TRAPPING AND MANIPULATION OF NANO-SIZED OBJECTS

In principle, all of the above techniques that have so far proved useful for micron-sized objects such as cells could be useful for nano-sized objects, especially if the nanowires or nanotubes could be used as the electrodes themselves.

5.1. Latex Beads

Latex beads have been used extensively in order to test various aspects of dielectrophoresis because they are robust and can be fluorescently labeled, and hence imaged. Furthermore, they are readily available in a variety of sizes from 10 μm to 10 nm.

The Fuhr group in Germany has been able to trap aggregates of 14-nm latex beads, aggregates of viruses of diameter around 100 nm, as well as single latex beads down to 650 nm in size [23, 24]. Subsequently the Morgan group in England achieved trapping of single 93-nm latex beads in 1998 [25, 26]. Green and Morgan used planar microelectrode arrays to separate a mixture of 93-nm and 216-nm latex beads into their constituent components [27].

In 1999, Hughes and Morgan separated unlabeled and protein-labeled 216-nm latex beads [28]. The dielectrophoretic properties of these beads were carefully modeled in [29, 30]. A detailed study of the DEP response of latex beads as a function of electrolyte composition and conductivity, electric field frequency, and particle size for 93-, 216-, and 282-nm latex beads was presented in [31]. The use of latex beads has been and continues to be a good testbed for the use of DEP in manipulating micro- and nanoparticles.

5.2. Molecular Dielectrophoresis

One of the most promising applications of dielectrophoresis in nanotechnology is the possible electronic manipulation of individual molecules. Later in this chapter we discuss the applications such an achievement would enable, such as massively parallel nanomanufacturing of new materials, one molecule at a time, with tailor-designed electronic, optical, magnetic, and mechanical properties. However, to date the clear demonstration of the manipulation by dielectrophoresis of a single molecule has not been achieved for any molecule less than 100 nm in size. A large reason, as discussed in Section 2.4, is that (to date) the thermal Brownian force dominates the dielectrophoretic force for such small objects.

While such an achievement may be possible in the future, it is still true that the nonuniform ac and dc electric fields establish *some* force, which, even though less than the thermal Brownian motion, will still cause a tendency for molecules to move in a certain direction, depending on the geometry of the electrodes. The quantitative study of these effects has been termed "molecular dielectrophoresis" [2].

To date all studies of molecular dielectrophoresis have used positive dielectrophoresis: the DEP force tends to push the molecules toward regions of higher electric fields. The geometry which has been studied almost exclusively is that of two concentric cylinders with the molecules dissolved in a solution in between the cylinders. If the density of the molecules as a function of the radial distance changes, this changes the dielectric constant as a function of the radius, and hence the capacitance from the inner to the outer cylindrical electrode.

In 1954, Debye and co-workers used dc dielectrophoresis of polystyrene (molecular weight 600,000) in cyclohexane [91, 92]. They used a dc non uniform electric field in a cylindrical geometry and monitored the capacitance change by measuring the shift in the resonant frequency of an LC circuit; similar studies were carried out by Prock and McConkey in 1960 [93].

In 1955, Lösche and Hultschig [94] used ac dielectrophoresis to study nitrobenzene in carbon tetrachloride, and poly(vinyl acetate) in nitrobenzene; however, both have permanent (instead of induced) dipoles. In 1973 Eisenstadt and Scheinberg [95, 96] studied dielectrophoresis and measured the diffusion constant of the biopolymers poly-γ-benzyl-L-glutamate (PBLG, M.W. $\approx$ 120,000) and poly-n-butyl isocyanate dissolved in ethylene dichloride (EDC);

both have permanent dipoles. By measuring the time dependence of the concentration change of the PBLG concentration due to the dielectrophoretic force, Eisenstadt and Scheinberg were able to determine its diffusion constant.

Thus, while the manipulation of a single nanomolecule is still not yet achieved, the ability to affect the concentration of large numbers of nanoscale molecules in solution with dielectrophoresis has been demonstrated over 30 years ago, giving hope to the use of nanodielectrophoresis at the single molecule level.

5.3. Conducting Nanoparticles

5.3.1. DC Dielectrophoretic Trapping

The basic principle of dielectrophoresis applies regardless of whether the field is dc or ac. (For example, the first recorded instance of dielectrophoresis was dc dielectrophoresis in 600 B.C., as discussed in Section 2.) Furthermore, Pohl calculated that metal balls in water would have the largest dielectrophoretic force of many different possible particle/solvent combinations [2]. In 1997, Bezryadin and Dekker combined these two ideas and used (positive) *dc dielectrophoresis* to trap 20-nm Pd nanoparticles between lithographically fabricated electrode gaps of about the same distance, that is, 20 nm [97, 98]. The Pd nanoparticles were dissolved in water. Bezryadin applied 4.5 V dc between the gaps, and then investigated the samples with a scanning electron microscope (SEM) after drying. The SEM images showed clearly the presence of one or a few nanoparticles bridging the gap between the electrodes, and this was confirmed by measuring the electrical resistance between the electrodes.

5.3.2. Pearl Chains

Particles undergoing dielectrophoresis often exhibit mutual attraction. This is due to the fact that dielectrophoresis involves an induced dipole moment in each particle, and dipoles interact and form what are called "pearl chains." The tendency of a group of particles in a field to form lines has been known for over two hundred years [2, 99]. This is, for example, responsible for the behavior of electrorheological fluids [100]. Pohl also studied this effect extensively in his experiments in cells [2]. In 1999, Bezryadin et al. observed this pearl-chaining phenomenon in conducting graphite nanoparticles ($d = 30$ nm), and named it self-assembled chains [101]. They used dc dielectrophoresis with the nanoparticles dissolved in toluene, and applied 40 V across a gap of 1 μm between Cr and Pt electrodes. They were able to pass current through this pearl chain of nanoparticles, and furthermore observed Coulomb gap (single electron transistor) behavior at temperatures all the way up to 77 K, because the capacitive charging energy of the nanoparticles was still comparable to the physical temperature even at 77 K.

5.3.3. AC Dielectrophoresis

In 2002, Amlani and co-workers used positive *ac dielectrophoresis* to trap 40- to 100-nm gold nanoparticles between a lithographically fabricated 60-nm gap between two gold electrodes [102]. The gold nanoparticles were dissolved in water, and a 2.5-V p-p ac voltage between 1 and 10 MHz is found to provide a yield of 100%, much higher than the yield if a dc dielectrophoresis is used. These structures were found to conduct electrically when a single gold nanoparticle was trapped, with a resistance of 3 kΩ. In a second experiment, prior to the dielectrophoretic trapping, the gold electrodes were coated with a self-assembled monolayer of 1-nitro-2,5-di(phenylethynyyl-4*-thioacetyl)benzene, a compound similar to one previously studied using a nanopore configuration and found to exhibit negative differential resistance [103]. In the dielectrophoresis experiment of Amlani, the current flow was presumably electrode-molecule-nanoparticle-molecule-electrode. Amlani and co-workers also observed negative differential resistance at room temperature, presumably due to the intrinsic electronic properties of the molecules in the self-assembled monolayer.

5.3.4. From Nanoparticles to Nanowires

In 1999, Velev and co-workers developed a biosensor which is chemically selective based on gold nanoparticles and latex micron-sized beads. The latex beads (suitably chemically functionalized) were assembled into a "pearl chain" wire between two electrodes with positive dielectrophoresis. The target molecules would then bind with immunoactive sites on the latex particles, and then a further set of chemically functionalized gold nanoparticles would bind to the target molecules. Then a silver enhancer is introduced to complete the circuit. The net result is a large change in conductance if and only if the target molecule is present above some minimum threshold in the test solution.

Later work by the same group used dielectrophoresis to directly assemble microwires from gold nanoparticles [104]. They found that 10- to 15-nm gold nanoparticles in solution, when subjected to 50- to 200-Hz electric fields by electrodes spaced apart by a few millimeters, grew wires of micron size and conducted electricity. This is analogous to the pearl-chain formation discussed earlier.

5.4. DNA

5.4.1. Washizu and Co-Workers

Starting in 1990, Washizu and Kurosawa began studies on DNA which showed that it is indeed possible to use dielectrophoresis to manipulate DNA [105]. They used the electric field produced between two parallel, thin-film aluminum electrodes (thickness 1 μm, spacing 60 μm) to "stretch" DNA molecules. When large concentrations of DNA molecules are used, they form bands due to the complicated and poorly understood DNA–DNA interactions. When low concentrations of DNA are used, one can see individual DNA molecules through fluorescence, and it is clear that the electric fields "stretch" each individual molecule out. The field strength used is approximately 10^6 V/m, and the frequency is varied from 40 kHz to 2 MHz, with only slight frequency dependence of the effect. Washizu and co-workers studied λ phage DNA (48.5 k base pairs, kbp), so that fully stretched they were about 17 μm long.

It is not clear from that data whether the ac electric field needs to be nonuniform for the stretching. It would be an interesting experiment to determine whether DNA is

stretched in uniform electric fields. Finally, they showed that it is possible to attach DNA to electrodes, which they interpret as being due to positive DEP: Near the edges of the thin electrodes, the electric field gradients are large, hence the DNA is attracted there. Once attached to the Al electrode (in this experiment, only one end is attached), it is bound chemically and remains, even after the electric field is switched off. In Figure 8, the results found by Washizu and co-workers are indicated schematically.

In 1995, Washizu and co-workers described several possible applications of this technique [106]. First, they described an optical/DEP technique to size-sort long DNA (with length greater than 10 kb pairs), which is difficult for conventional gel electrophoresis. This was demonstrated with λ phage DNA (size 48.5 kbp). Second, they measured the activity rate of exonuclease digestion of DNA, by measuring the double strand length as a function of time during digestion. DNA lengths of order 10 μm can be measured because DEP caused the DNA to be stretched out. (They found that single strands of DNA are not stretched by DEP.) A further method was developed to stretch DNA molecules and position them at two different electrodes, using a combination of a floating electrode geometry and also chemically treated (biotin and avidin) electrodes. For unknown reasons, without the floating electrode geometry it was possible to attach one end of a DNA molecule to one electrode, but not the other end to the other electrode. Apparently, the high electric fields near the electrode induced currents away from the electrode, preventing the second end of the DNA molecule from binding, but not the first end.

The DNA so immobilized is shown to still be biochemically active. In 1993, Banata and co-workers used the DEP technique to attach one end of DNA to an aluminum electrode; the other end was free but stretched out with DEP. Just after turning off the electric field, and before the DNA had a chance to re-coil, they imaged single fluorescently labeled RNA polymerase molecules sliding along the DNA [107]. The technique was used to study the DNA–protein interaction with other proteins (*Pseudomonas putida* CamR) in 1999 [108]. Future applications of this technique

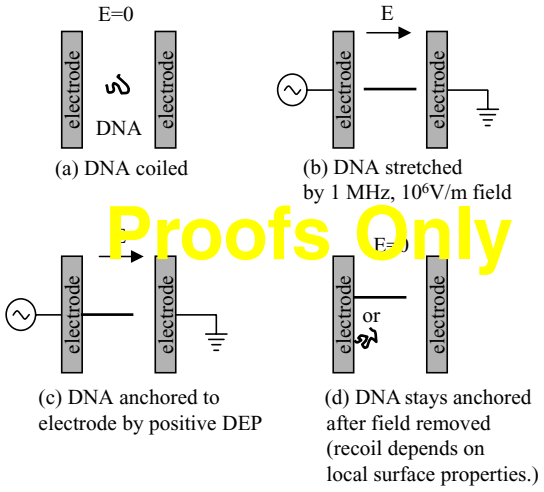

Figure 8. Schematic representation of the findings of Washizu and co-workers.

may lend insight into DNA–protein interactions in general, and the regulation and control of genetic expression in particular.

In 1999 Ueda and co-workers studied the DEP stretched DNA molecules with AFM, after drying the solvent (water). They concluded that the DEP stretched and trapped molecules do not aggregate but in contrast are trapped individually [109].

In 2000, the Washizu group used dielectrophoresis and floating electrodes to attach both ends of λ phage DNA molecules to aluminum electrodes [48, 110], using the floating electrode technique described above. In this work, they etched the glass slide below the gap between the electrodes so that the DNA was freely suspended. (Although it has gone largely unnoticed by the MEMs community, this technique to assemble freely suspended DNA should have many applications in nanomechanical systems made of DNA.) Since the DNA was freely suspended in solution there is no issue of steric hindrance of biochemical activity. Then, in a further set of experiments [48], they used optical tweezers to manipulate 1-μm latex spheres labeled chemically with the digestive enzymes DNaseI (which has no base pair selectivity) and HindIII (a restriction enzyme which cuts DNA at only specific base sequences). They were able to bring the bead up to the DNA. In the case of DNaseI, the DNA was immediately cut. In the case of HindIII, the bead was moved up and down the DNA until it matched the correct sequence, at which point it was cut.

In 1998, the Washizu group studied the polarization of the fluorescent emission from dielectrophoretically stretched DNA [111]. The polarization of the emitted light was quantitatively measured and correlated with the applied electric field intensity, as well as the pH of the solution. Several interesting results were obtained, indicating that the counterion cloud surrounding the DNA molecules has a large influence on the stretching of DNA by electric fields. The details of this influence are still not fully understood. Many of these results from Washizu and co-workers are reviewed in two book chapters [112, 113].

5.4.2. Asbury and Co-Workers

In 1998, Asbury and van den Engh were able to use dielectrophoresis to trap DNA with a floating electrode geometry: The electric field was applied from external electrodes; floating gold electrodes spaced by 30-μm gaps concentrated the electric field, which served to trap the DNA [114]. They also studied λ phage DNA in D.I. water, but used gold electrodes (thickness 40 nm), and audio frequency (30 Hz) fields. As in the Washizu experiments, the DNA underwent positive dielectrophoresis: it was attracted to regions of high electric field intensity, which occurs near the edges of the electrodes. Asbury used much lower frequency voltages (typically 30 Hz) than Washizu, and found no stretching of the DNA at these frequencies. Furthermore, Asbury found that the DNA did not become stuck to the gold electrodes, in contrast to Washizu's experiments where the DNA did become stuck to aluminum electrodes.

Regarding the frequency, at dc no more than roughly 1 V can be applied across an electrode/water interface; otherwise electrolysis followed by bubbling can occur. Washizu found

that much larger voltages could be applied as the frequency was increased from 1 kHz to 1 MHz (they did not study frequencies below 1 kHz). In Asbury's experiments, the gold electrodes were floating, but there was still less than 0.5 V between each (floating) electrode pair, so that electrolysis did not occur. Asbury's experiments found that DNA could be trapped in deionized water, but not in isotonic saline. They estimate that the force on the DNA was in the femtonewton range. Since the DNA molecules were not stuck to the gold electrodes, Asbury was able to simultaneously apply a dc field and move the stretched DNA molecules with electrophoresis.

In 2002, Asbury and co-workers continued this work by integrating it with a simple microfluidic device, fabricating a 15-μm-wide PDMS channel on top of gold electrodes which, in contrast to their earlier work, were electrically contacted (not floating) [115]. With the gold electrodes and 30-Hz voltages of roughly 3 V p-p, they were able to trap DNA and then release it using positive dielectrophoresis. Their estimates show that 50% of the DNA introduced into the microfluidic channel was trapped.

Asbury found the trapping "efficiency" to decrease with increasing frequency between 5 Hz and 2 kHz, with an effective time constant of 3 ms. The origin of this frequency dependence is attributed to the distortion of the counterion clouds that surround the DNA molecules in solution, although the details of this effect are currently poorly understood.

5.4.3. Ueda and Co-Workers

In 1997 Ueda et al. used much-lower-frequency ac electric fields, and studied the electronic dielectrophoretic stretching of DNA in polymer laden solutions. They found the polymer (polyacrylamide) assisted the stretching of DNA for applied electric fields in the frequency range of 0.1 to 100 Hz [116]. They found this stretching to occur at field strengths as low as 10^4 V/m; no net motion of the DNA was reported.

5.4.4. Chou and Co-Workers

In another work with floating electrodes, Chou and co-workers used *insulating* posts fabricated with micromachining techniques, and electrodes external to the device [117]. The slightly conductive solution served to enhance the electric field near the gaps between the posts, and DNA was found to be trapped there for voltages on the electrodes of roughly 1000 V and frequencies between 50 Hz and 1 kHz. The corresponding electric field strength was 10^5 V/m. In this work, the DNA was apparently not stretched at all, presumably because of the constricted geometry used. In contrast to the work of Asbury, Chou found that the trapping force increased with increasing frequency, and also calculated that the trapping force was roughly 1 fN.

5.4.5. Tsukahara and Co-Workers

In recent work [118], Tsukahara and co-workers studied dielectrophoresis of single DNA molecules using frequencies between 1 kHz and 1 MHz and field strengths around 10^4 V/m, using quadrupole electrode patterns similar to those shown in Figure 3. They found that the DNA underwent positive dielectrophoresis (i.e., it was attracted to the high field regions near the edges of the electrodes) for frequencies between 1 kHz and 500 kHz, and negative dielectrophoresis between 500 kHz and 1 MHz, in contrast with the findings of previous work. This is to date the only reported observation of negative dielectrophoresis of DNA; the discrepancy may be related to the different solvents used, although at this point it is still an open question. Furthermore, Tsukahara and co-workers used electric fields that were roughly a factor of 10 smaller than previous workers, and still were able to observe the dielectrophoretic forces on a single DNA molecule. This may again be due to the solvent used, or the fact that Tsukahara used a quadrupole electrode geometry, which is different than previous works. Additionally, Tsukahara did not observe any stretching of the DNA with the application of an ac electric field.

5.4.6. Porath and Co-Workers

In 2000, Porath and co-workers used positive dc dielectrophoresis to putatively trap 10-nm-long poly(G)-poly(C) double strands of DNA between Pt electrodes with 8-nm spacing [119]. Through a series of control experiments, Porath concluded that the trapped object was indeed DNA, and that its electrical properties were semiconducting. Many other researchers up to and since then have considered the electronic properties of DNA as a molecular wire. The issue is still under investigation [120].

5.4.7. Summary

The detailed mechanisms for the frequency dependence, electric field dependence, concentration dependence, pH and ionic dependence of the dielectrophoretic manipulation of DNA are still not explained in a systematic, quantitative way, and many of these dependences have yet to be quantitatively measured. However, it is clear now that it is possible to use dielectrophoresis to manipulate DNA under a variety of conditions and frequencies. This knowledge could be used in a variety of contexts, including lab-on-a-chip diagnoses and genetic expression profiling, as well as electronic methods of controlling DNA chemistry. This latter possibility has the potential to provide a new nanomanufacturing technology based on both chemical self-assembly techniques and integrated, massively parallel, economical electronic control of the same.

5.5. Viruses

5.5.1. Influenza

To date two different research groups have succeeded in trapping at least four different species of virus with dielectrophoresis. The first group to trap viruses was that of Fuhr and co-workers in 1996 [121]. They used quadrupole, three-dimensional traps to trap fluorescently labeled influenza viruses ($d \approx 100$ nm) using negative dielectrophoresis traps, and 1-MHz electric fields with field strength around 10^5 V/m. (The gap between electrodes was approximately 5 μm with 11-V p-p voltage.) They also trapped 14-nm latex beads. In these experiments, the viruses formed aggregates in the centers of the traps. In later work with similar geometries, fields, and frequencies, the same group was also able to trap Sendai viruses into aggregates as well [122].

5.5.2. Tobacco Mosaic

In later work, Morgan and co-workers used interdigitated electrode fingers spaced by 4 μm with saw-tooth shapes to manipulate tobacco mosaic viruses [123, 124]. The tobacco virus is rod-shaped, with length of 280 nm, and width of 18 nm. Morgan used field strengths of roughly 10^6 V/m, and varied the frequency between 1 kHz and 2 MHz. Although they were not able to observe individual virions, they could see a faint haze as the density increased or decreased in response to the applied electric field. They found both positive and negative dielectrophoresis, depending on the frequency used. Positive dielectrophoresis was observed for frequencies below about 1 MHz, and negative dielectrophoresis for higher frequencies. The crossover frequency was very dependent on medium conductivity, which was varied between 2×10^{-3} and 10^{-1} S/m by varying the potassium phosphate buffer concentration.

5.5.3. Herpes

In 1998, Hughes and co-workers used planar quadrupole traps such as the one shown in Figure 3 with 6-μm gaps to trap Herpes simplex viruses, which are spherical with diameter of about 250 nm [125]. They studied dielectrophoresis of the virus with frequencies from 10 kHz to 20 MHz, and observed negative dielectrophoresis for frequencies above about 5 MHz. The field strengths required for the trapping were about 10^6 V/m. Later work by the same group found that the crossover frequency between positive and negative dielectrophoresis for the herpes virus was very dependent on the medium conductivity in the range between 10^{-4} and 10^{-1} S/m, and this dependence was strongly affected by the presence or absence of manitol [126, 127].

5.5.4. Virus Separation

Using the results from their previous studies, Morgan and co-workers studied both tobacco and herpes virus in the same solution, using quadrupole electrode geometry [124, 128]. At 5 MHz, the herpes virus experiences negative dielectrophoresis and is collected in the center of the quadrupole. In contrast, at 5 MHz the tobacco virus experiences positive dielectrophoresis and is collected at the edges of the quadrupole geometry. Thus, two different virus species were physically separated due to their different frequency response to dielectrophoresis.

5.6. Proteins

A protein consists of a long chain of subunits (amino acids) which are folded into very complicated three-dimensional structures; the structure is closely related to the function. Most proteins of biological significance are around 1–10 nm in physical size. All species of life are based on only 20 common amino acids [129]. The modern field of *proteomics* seeks to understand, categorize, and tabulate all proteins useful for life [130].

There have been several studies of the effects of moderate electric fields and strong pulsed fields on the conformational state of proteins such as the helix-coil transition [131]. Reviews of the dielectric properties of biopolymers, dealing predominantly with linear response, low field behavior, are given in [3, 4, 132–134]. However, given the importance of protein chemistry in modern molecular biology, it is surprising how little work to date has been performed on the interaction between strong electric fields and proteins.

5.6.1. Protein Trapping

In 1994, Washizu and co-workers studied the effect of dielectrophoresis on the following proteins: avidin (M.W. 68 kDa), concanavalin A (M.W. 52 kDa), chymotripsinogen A (M.W. 25 kDa), and ribonuclease A (M.W. 13.7 kDa) [84]. These proteins have diameters ranging from 1 to 5 nm. In this series of experiments, they used aluminum (thickness 1 μm) electrodes in an interdigitated, castellated geometry with gaps ranging from 4 to 55 μm. The solvent was D.I. water. They used fluorescence to observe the positions of the proteins. They observed excess fluorescence near the electrodes (i.e., near the high field regions), so that they observed positive dielectrophoresis. They knew it was DEP because they found a dependence on the field strength, not the voltage, by using different gaps between the electrodes.

According to rough estimates of the DEP force for their electrodes (a quantitative calculation was not performed), the thermal Brownian motion should overwhelm the DEP force so that nothing should be observed. And yet they observed increased fluorescence in the high field regions. This can be interpreted one of two ways: first, that we do not understand why DEP works so well on proteins; second, that the proteins are accumulating and the agglomerate acts as an effectively large polarizable particle that is less susceptible to Brownian motion and can be trapped.

Washizu argues that the second explanation (agglomeration) is not occurring because when they change the initial concentration by a factor of 10, the time to form the "aggregation" does not vary much, and this is inconsistent with a simple aggregation model of dipole–dipole attraction. Dipole–dipole attraction goes as d^{-4}, so that the time to form the agglomeration should vary as the density n^4.

If an optical setup with enough sensitivity to image a single fluorescing protein [135] could be achieved, this issue could be resolved. Washizu was able to demonstrate that trapping of various sized proteins depends on their molecular weight, so that separation of chemical species of various sizes could in principle be observed for applications in nanobiotechnology. Thus a "single molecule fluorescence" experiment, if it could be performed, would be definitive proof the DEP can be used with 10^6 V/m to manipulate 1- to 5-nm proteins.

In more recent work, Kawabata and Washizu [136] developed a biosensor for the protein AFP (alpha-fetoprotein, 70 kDa), an important diagnostic protein, which is detected in the serum of a liver-cancer patient. There, they used the DEP properties of proteins (antigens and antibodies) as well as 150-nm latex beads with antibodies immobilized on the surface. This is an example of an important point: even though we have organized this review according to the types of nano-objects that can be manipulated with DEP, the application of DEP to a heterogeneous population of objects could provide even more applications than just manipulating one type of object at a time.

5.6.2. Protein Folding

The previous section discussed primarily controlling the location of proteins with dielectrophoresis. However, given that the conformational state of a protein is related to its function, it is natural to consider whether an applied electric field can change a protein's conformational state, and possibly even unfold the entire chain of amino acids into a straight line, as Washizu was able to do with DNA. While the latter is still unproven experimentally, Washizu and coworkers have shown that it is indeed possible to use electric fields to change the conformational state of a certain protein, the flagellum of a bacteria.

The flagellum of certain types of bacteria consists of a single, spiral shaped protein about 20 nm wide and 10 μm long. When it is rotated it acts as a corkscrew, propelling the bacteria forward. However, other conformational states of the amino-acid chain are possible; three in particular are called "straight," "curly," and "coiled." Because the flagellum is a long protein, its conformational state can be directly observed under a microscope, if fluorescently labeled.

Washizu and co-workers found that ac electric fields of roughly 10^6 V/m could transform flagella from one conformation state to another [112, 113, 137]. Furthermore, they found this process to be *reproducible and reversible*, observing no permanent damage to the flagella after application of the electric field.

Similar work on the electric field-induced conformation changes in other proteins (e.g., poly-(L-lysine) and poly-(L-glutamic acid)) has been reviewed in [134]. There, the work described involves measurements of optical dichroism as a function of applied electric field pulses. The optical dichroism is also strongly affected by electric field-induced orientation, making it difficult to conclusively demonstrate electric field-induced conformational changes in protein structure.

This relatively unexplored area has great potential for the future. By electronically controlling the conformational state of proteins, it may be possible to electronically control their biological function, or even to engineer new functionality into existing or tailor-designed proteins. This future molecular nanotechnology could have broad applications, which will be discussed toward the end of the review, and could also allow for further scientific studies of the process of protein folding.

5.7. Carbon Nanotubes

5.7.1. Nanotubes in Solution

Several research groups have successfully used dielectrophoresis to manipulate carbon nanotubes in solution. The general procedure is similar to that of Washizu's manipulation of DNA, with the exception that nanotubes are known to be good conductors. Most experiments demonstrating manipulation of carbon nanotubes in solution are a variation of the general process depicted schematically in Figure 9.

Nanotubes are not known to be soluble in any solvent, but can be dispersed by sonication. Once dispersed, a drop of the solution can be placed onto microfabricated electrodes as shown in Figure 9A. Next, either a dc or an ac voltage is applied. This serves two purposes. First, it induces a dipole moment in the carbon nanotube, and this dipole

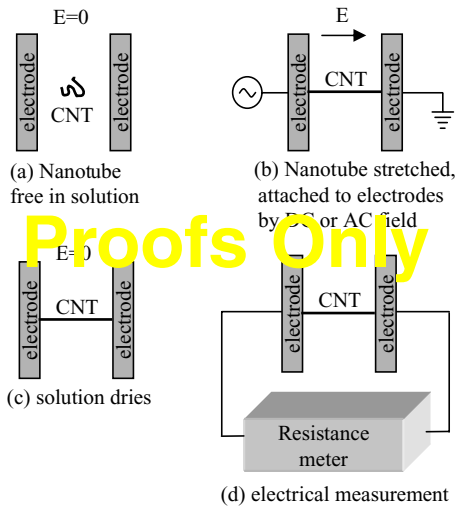

Figure 9. Schematic representation of the manipulation of carbon nanotubes in solution.

experiences a torque, given by Eq. (10). This torque tends to align the nanotube with the axis of the electric field. The electric field need not be nonuniform for this alignment, but to date experiments have not tested the dependence of the alignment on the uniformity of the field in any quantitative fashion.

Simultaneously, the induced dipole [138] in the nanotube experiences a force given by Eq. (2). (Equation (3) is not directly applicable as it assumes a spherical particle.) To date all measurements on carbon nanotubes have found that they undergo *positive* dielectrophoresis; that is, they are attracted to regions of high electric field strength. This can be exploited to electrically contact nanotubes: the electrodes which generate the electric field gradient can also be used as electrical contacts to the nanotube. This is indicated schematically in Figure 9D.

When water is used as the solvent (which is desirable for biologically interesting measurements), as discussed above, the applied voltage to the electrodes should be less than 1 V to avoid hydrolysis (and hence bubbling). By using ac voltages, as Washizu et al. found in 1990 [54], the applied voltage (hence electric field strength) required for hydrolysis increases with increasing frequency. If one is willing to use an insulating solvent, then the applied voltage (hence electric field) can be much larger, even at dc. Pohl, for example, used commonly used applied (ac) voltages of thousands of volts with insulating solvents such as organic solvents and CCl_4 [2].

5.7.2. DC Dielectrophoresis and Electrophoresis

The first dielectrophoretic manipulation of nanotube ropes was done using dc dielectrophoresis in 1997 by Bezryadin and Dekker [97]. Bezryadin used cyclohexane as the solvent, and a dc voltage of 4.5 V between AuPd electrodes spaced by 150 nm. He simultaneously measured the dc current flowing between the electrodes, and was able to see an electric current flow as soon as a nanotube rope was trapped.

Bezryadin found that the trapping was effective, but the nanotube ropes were not aligned parallel to the electric field. This is possibly due to the fact that the length of the trapped ropes was much larger than the gap between the electrodes.

When a dc electric field is used, if the object is charged it will respond to the electric field via conventional electrophoresis. A simple way to test whether the nanotubes are charged and experiencing electrophoresis or neutral and experiencing dielectrophoresis is to observe whether they preferentially move toward the cathode or anode or neither. If the nanotubes do not preferentially conglomerate at one polarity, then the effect is dielectrophoresis. Apparently in Bezryadin's experiments, the nanotubes behaved as neutral objects, and underwent dielectrophoresis. However, in two other experiments, multiwalled nanotubes (MWNTs) are found to behave as positively charged, conglomerating at the cathode [139], and negatively charged, conglomerating at the anode [140]. (Chen et al. found that single-walled nanotubes (SWNTs) also conglomerated at the anode under a dc electric field [141].) These discrepancies may indicate that the electrical properties of nanotubes are sensitive to the chemistry of the solvent. This effect, if it can be further characterized and explained, could prove very useful in nanomanipulation of nanotubes with electric fields in solutions.

5.7.3. AC Dielectrophoresis of MWNTs

In 1998, Yamamoto and co-workers studied the effects of ac electric fields on MWNTs of lengths between 1 and 5 μm, and diameter 5–20 nm, using Al electrodes with 400-μm gaps and field strength of 2×10^5 V/m [142]. The MWNTs were dispersed in isopropyl alcohol. They found that the nanotubes were both *aligned* and attracted to the electrodes (i.e., underwent positive dielectrophoresis) for ac frequencies between 10 Hz and 10 MHz. Yamamoto and co-workers found that the degree of orientation of the nanotubes increased with increasing frequency, and with increasing nanotube length. Furthermore, they found that graphite impurities had a different frequency-dependent response to the ac electric field, which may be important technologically in separating nanotubes from impurities. Yamamoto also found that the alignment was more effective with ac dielectrophoresis than with dc dielectrophoresis [139], consistent with the findings of Bezryadin. A complementary technique of optical polarization measurements showed that ac electric fields could align nanotubes dispersed in ethanol [143].

5.7.4. AC Dielectrophoresis of SWNTs

In 2001, Chen and co-workers carried out a similar study of the effects of ac electric fields on SWNTs dispersed in ethanol [141]. They applied fields of 5×10^6 V/m in the frequency range from 500 Hz to 5 MHz. They found the SWNTs to be oriented more strongly at higher frequencies, and they found the SWNTs experienced positive DEP for all frequencies studied. They also found no alignment effect from a dc electric field. Thus SWNTs and MWNTs appear to behave similarly under intense ac electric fields.

The first application of ac dielectrophoresis to attach two ends of SWNTs was reported in an e-print in early 2002 [144]. The authors used Ag and Au electrodes spaced by 100 nm to trap ropes (bundles) of SWNTs dispersed in N,N-dimethylformamide (DMF). They found the nanotubes formed electrical contact with the Ag electrodes, but not the Au electrodes. The trapping was effective for frequencies between 1 kHz and 1 MHz, at applied fields of 10^7 V/m. Krupke was also able to simultaneously measure the ac resistance between two electrodes for the 1-kHz trapping experiments, allowing real-time monitoring of the trapping.

Nagahara et al. found similar results [145], trapping SWNT bundles with gold electrodes spaced by either 20–80 nm or 20 μm, and applying 1 MHz and dc electric fields of strength 10^7 V/m. They found that the dc fields trapped bundles of SWNTs and graphite impurities, whereas the ac fields trapped only nanotube bundles. They were also able to electrically measure the current through the nanotubes after drying the Triton solvent.

Diehl and co-workers have taken this process one step further, and fabricated cross-bar structures by first aligning and immobilizing SWNT ropes in one direction and then, aligning and immobilizing nanotube ropes in a perpendicular direction [146]. The distance from one rope to the next was not determined by the lithography, but rather the chemical control of the coulombic interactions between the tubes and between the ropes. Diehl's experiments used frequencies between 10^4 and 10^6 Hz, with very little frequency dependence. The solvent consisted of a mixture of ortho-chlorobenzene and $CHCl_3$. (The field strength was not reported.) This represents an initial step toward one of the ultimate goals of self-assembled systems and nanotechnology in general: nonlithographic, economical, massively parallel manufacturing of electronic circuits on the nanoscale.

While to date there has been no reported trapping of an individual SWNT between two electrodes (as opposed to a bundle), such an achievement does not seem unreasonable to expect in the near future.

5.7.5. Controlling Nanotube Growth

Chemical vapor deposition (CVD) of carbon nanotubes is a promising new technique for the growth of high-quality single- and multiwalled carbon nanotubes [147]. The nanotubes grow from catalyst sites that can be lithographically defined on a chip [148]. However, the *direction* of the nanotube growth from these lithographically patterned catalyst sites is generally random, an issue that needs to be solved before massively parallel integrated nanotube circuits can be realized.

One possible technique to control the direction of nanotube growth is to apply an electric field (dc or ac) *during* the growth. The electric field will induce a dipole moment in the (growing) nanotube, which will experience a torque (see Eq. (10)), hence becoming aligned with the electric field. This technique was first applied to the growth of vertically aligned MWNTs in 2001 by Avigal and co-workers [149].

Later work by Zhang and co-workers [150] used both dc and ac (5 MHz) electric fields to direct the growth of SWNTs parallel to the substrate. The field strengths used were 5×10^5 V/m, and freely suspended SWNTs up to 40 μm in length were grown. The fields were generated between thin-film electrodes which were electrically contacted during growth. Later work by the same group achieved aligned

nanotube growth where the end result was a SWNT immobilized on the surface of the substrate [151].

5.7.6. Nanotubes as the Electrodes

Ultimately, for nano-DEP, one wants the smallest gap possible, and the smallest electrode radius of curvature possible. We would like to suggest that one way to achieve this would be to use nanotubes themselves as the electrodes. Very high electric field gradients should be possible [32].

5.8. Nanowires

5.8.1. Metallic Nanowires

In 1999, van der Zande and co-workers studied the orientation effects of uniform electric fields on 15-nm-diameter gold rods of lengths 39–259 nm in water using optical polarization techniques [152]. They found that, for an applied field strength of 10^5 V/m and an applied frequency of 10 kHz, significant orientation of the gold nanorods could be achieved.

Later work by Smith and co-workers studied gold nanowires down to 35 nm in diameter, although most work was performed in 350-nm-diameter wires of several microns in length [153]. Smith and co-workers used a combination of floating and electrically contacted electrodes, field strengths of up to 10^7 V/m, and frequencies from 20 Hz to 20 kHz. They found strong orientation effects and positive dielectrophoretic trapping of the nanowires to the floating electrodes for frequencies above 200 Hz; higher frequencies were most effective. Due to the floating electrode geometry used, the process was self-limiting: as soon as one wire bridged a particular pair of floating electrodes, it would short out the capacitively induced voltage on that pair of floating electrodes, preventing further trapping across that pair. Post manipulation lithographic contact to the floating electrodes showed the nanowires to be in good electrical contact with the trapping electrodes.

5.8.2. Semiconducting Nanowires

In 2001, Duan and co-workers used dc dielectrophoresis to align and electrically contact InP nanowires (d = 30 nm) [154]. There, electric field strengths of 10^7 V/m were applied from electrodes spaced by 25-μm gaps. The solvent used was chlorobenzene, so that electrolysis was not an issue. (DC voltages of 100 V were used.) By selectively energizing different pairs of electrodes, Duan was able to align InP nanowires into a cross-bar topology using layer-by-layer application of dielectrophoresis.

6. APPLICATIONS

6.1. Molecular Electronics

Recent work of Chen, Reed, and co-workers [103, 155, 156] has investigated the conducting properties of layers of molecules. The investigation of electronic properties of molecular conductors has been termed *molecular electronics*. The use of lithography alone will not allow for the controlled, rational design and fabrication of single molecule conductors.

One possible application of nanodielectrophoresis is the controlled placement of individual molecules for molecular electronics. If nanotubes and nanowires can be used themselves as the electrodes (and then as the interconnects), our calculations [32] show that it should be possible (based on the scaling consideration presented in Section 2.4) to trap individual molecules as small as 1 nm.

In Figure 10, we show one possible application of our proposed nanotube trapping scheme. An electrically contacted nanotube is cut with an AFM, then a large ac voltage is applied. By the method of images, the electric field gradients are the same as a geometry where a nanotube is in close proximity to a large conducting plane; the field gradients of a reasonable voltage (1 V) on the nanoscale should be quite large, allowing us to trap very small objects, possibly even single molecules. Trapping of DNA at the ends of nanotubes does not seem to be out of the question, nor is it impossible to trap any other number of molecules for nanotube-electrode molecular electronics. This electronically assisted chemical self-assembly contains the ingredients for molecular transistors wired up with nanotube interconnects in a possibly massively parallel process for large-scale integrated molecular electronics ("LIME," if you will).

In Figure 11, we illustrate one possible application of this nano-trapping. 2′-amino-4-ethynylphenyl-4′-ethynylphenyl-5′-nitro-1-benzenethiolate (AEENBT) is used as a model [155]. Note that the hydrogen atom at the end bonded to sulfur can be replaced by other functional groups, for example, -$COCH_3$. Likewise, the protruding hydrogen atom farthest away from the sulfur atom can also be replaced by another group. By chemically selecting and optimizing the bridging molecule, in particular, the end functional groups, can one achieve ideal contact between the bridging molecule and carbon nanotubes?

Using Au as electrical contact, the Reed group [155] has made a molecular random access memory cell [156]. Multiple read write cycles were realized in a self-assembled monolayer film of AEENBT. The bit retention time was found to be of the order of 15 minutes. However, it is very difficult to combine lithography with 2-nm molecules. Nanodielectrophoresis uses the natural nanometer size of carbon nanotubes. With a defined carbon nanotube gap (2 nm) and diameter (1–2 nm), one will have a chance to electrically contact a single AEENBT.

Another potential advantage of trapping molecules with carbon nanotubes is the potentially better contact quality between carbon and other nonmetal atoms. Most molecule–metal junctions are poor circuit elements. The resistance

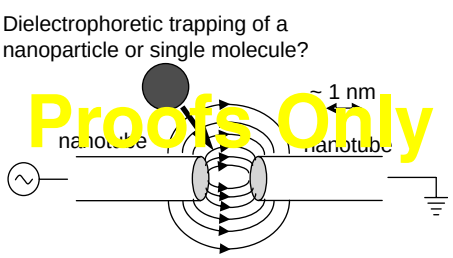

Figure 10. Schematic representation of an idea of how to trap 1-nm-sized particles or molecules.

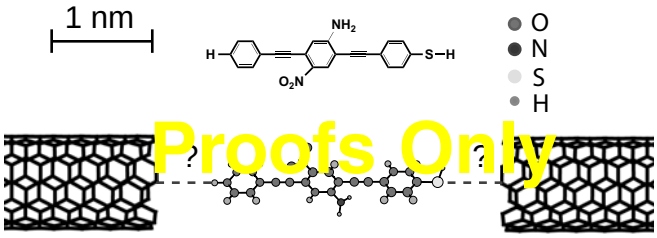

Figure 11. An overly simplistic schematic view of potential molecular electronics with carbon nanotubes assembled with nanodielectrophoresis. This technique could allow rapid investigation of many such schemes in a massively parallel fashion.

is usually of the order of 1 MΩ [157], which is far away from the ideal contact. One of the reasons is the different electronegativity between metals and nonmetals. For example, in a S–Au(Ag) junction, an interfacial dipole leads to a Schottky barrier in that sulfur is more electronegative than gold and silver. Carbon, which is also a nonmetal element, may prove better to contact molecules.[1] One can ultimately investigate more complicated geometries and architectures for integrated molecular electronic devices with nanotube interconnects.

6.2. Nanomanufacturing

Future applications of nano-DEP do not need to be limited to the manipulation of individual or small numbers of nanoparticles. Rather, it should be possible to scale up these nanomanipulation methods for massively parallel processing at the single molecule level. Even macroscopic quantities of materials could be fabricated one molecule at a time. New materials with tailor-designed electronic, optical, magnetic, and mechanical properties could go from nano-CAD design to reality in a matter of hours or minutes at very low cost. This integration would be a true synthesis of the top-down and bottom-up approaches to nanotechnology.

6.3. Nanomachines

Through rotating electric fields generated by microfabricated electrodes, it has been possible to rotate 5-μm latex beads and also cells in solution [8]. One could call such an apparatus a dielectric micromotor, where the electrodes are the stator and the rotating latex bead the rotor. Hagedorn et al. took this concept one step further and microfabricated a large variety of micro "rotors" out of Al and polyimide, which had dimensions of approximately 100 μm [158]. They were able to demonstrate rotor speeds of up to 3000 RPM.

Recently Hughes has presented a theoretical evaluation of the ultimate limits of rotor performance, using nano-DEP to drive rotors down to 1 nm across [159]. He concluded that a 1-μm-long by 100-nm-wide rotor should be able to generate a torque of 10^{-15} N/m, equivalent to that of a bacterial flagellar motor. Although he does not discuss how one might realize such a rotor, we suggest that using carbon nanotubes as both the rotor and stator is one feasible technique to realize this, since it is known that nanotubes can be contacted by external electrodes. Such a nanomachine would be a step toward Drexler's vision of molecular nanotechnology [160], proving Feynman's statement that "there's plenty of room at the bottom" [161].

6.4. Nanobiotechnology

The applications in nanobiotechnology are practically limitless. For example, Washizu has taken the first step toward DEP FFF of proteins [84], on *one* protein. It is natural to speculate that in the future, DEP FFF may find application in the ability to separate *all* proteins from the human proteome, uniquely based on their dielectric spectral properties. If enough sensitivity could be achieved, one could measure genetic expression of the entire human genome in a single cell. This could have numerous applications in drug screening and discovery.

One does not need to consider only passive, scientific or diagnostic-based measurement of biochemical activity. Nano-DEP has already proved capable of manipulating viruses. This leads one naturally to ask the question: Based in part on nano-DEP, can one design an active, electronically controlled artificial immune system? A nano-liver or a nano-kidney? The answer to this question is not yet known, but would have significant impact on humanity in general if it turns out to be "yes."

6.5. Nanochemistry

The force required to break a single chemical bond is roughly 1 nN [162]. Our calculations show that this can be the same order of magnitude that is generated by DEP on a micro- or nanoparticle, if nanotubes are used as the electrodes [32]. While to date AFM and SPM have been used for studying single molecule chemistry, it is also natural to speculate that nano-DEP experiments can be designed to electronically study and control the breaking of a single chemical bond.

7. UNANSWERED QUESTIONS

Although DEPs application in nanotechnology is still in its infancy, it can be considered a proven technique to electronically manipulate micro- and nanosized objects. However, the studies performed to date have left some key questions unanswered:

- What is the effect of Joule heating?
- What is the smallest molecule that can be trapped?
- What field strengths are needed for this?
- Since the forces depend on the field gradient only, is it possible to design different electrode geometries to achieve stronger trapping forces for a given applied voltage?
- Can trapping of individual macromolecules occur in biologically relevant solutions, fraught with conduction ions?
- What is the effect of molecule–molecule interactions on traps that hold more than one molecule?
- What is the role of electrohydrodynamics?

[1] We thank Shengdong Li for pointing this issue out to us.

Joule heating occurs due to current flow through the solution. This is especially a question in solutions of biological significance with ionic concentrations that can also carry current. The heating may cause connective fluidic currents which will overcome the dielectrophoretic forces. The amount of Joule heating is difficult to predict, since the conductive properties of the solution at MHz frequencies may not be known.

Macromolecules may not behave as bulk dielectrics, but have deviations from simple bulk behavior. These issues are difficult to address theoretically and more experiments need to be done to push DEP to the single molecule limit.

At the very high electric fields necessary for DEP to overcome Brownian motion of nanoparticles, the electric field may also interact directly with the fluid itself. The study of the interactions between electric fields and fluids is called electrohydrodynamics. Serious, concerted effort to understand electrohydrodynamics at the nanometer scale has only recently begun [163–169]. Understanding these effects will obviously have important implications for the applications and ultimate limits of nano-DEP.

The importance of these effects was made clear by Washizu et al. [106], who found that, while it was possible to stretch and attach DNA to one electrode, electrohydrodynamical effects prevented attaching the other end of the DNA molecule to a second electrode. Instead, a floating electrode geometry was needed to avoid the electrohydrodynamical effects.

The electrohydrodynamic effects of high electric fields at the nanoscale is a difficult problem to investigate both experimentally and theoretically, and will require considerably more effort to quantify, understand, and eventually control.

8. CONCLUSIONS

The use of dielectrophoresis has already found numerous applications in biotechnology, nanotechnology, and nanobiotechnology. Using conducting metal and carbon electrodes fabricated with either optical or electron beam lithography, coupled with modern microfluidic integrated circuits, it has been possible to manipulate, trap, separate, and transport DNA, proteins, viruses, cells of various types from many different species, including both plant and animal, metal nanoparticles, latex beads, carbon nanotubes, semiconducting and metallic nanowires, semiconducting nanoparticles, and quantum dots.

In order to bring this vast body of knowledge to fruition, several steps remain to be taken. First, the power and economy of massively parallel fabrication and manufacturing methods, as well as massively parallel operations on a single chip, have not yet been exploited. While the techniques described here are compatible with the processing techniques of modern semiconductor integrated circuits which achieve routinely millions of transistors on a chip at the cost of only a few dollars, to date most studies and demonstrations of nanodielectrophoresis have only been on a few or at most a dozen operations at a given time, such as the separation of viable and nonviable cells. These processes need to be integrated with each other, with microfluidics, and with existing silicon microelectronics technology for many (millions) of operations for a true, integrated lab-on-a-chip.

Second, new applications must be found for this massively parallel processing, manipulation, and manufacturing capability. To date the manipulation of nano-sized objects has traditionally been painstaking, expensive, and slow. If massively parallel techniques of nanomanipulation can be manufactured and made readily available, many new opportunities which harness this economy of scale will need to be imagined, designed, and realized, such as new materials and devices with tailor-designed electronic, optical, magnetic, and mechanical properties. By integrating these with biological and chemical functions, artificial cell, immune systems, tissues, and even organs may someday be designed, fabricated, and made readily and cheaply available to every human being on the planet, for medical applications such as point-of-care diagnostics, drug discovery, artificial immune systems, and ultimately the treatment and prevention of disease.

Third, and finally, the next step in size reduction must be taken in order to create a true nanomanufacturing technology. The origins of dielectrophoresis allowed the use of traditionally machined electrodes to manipulate micron-sized objects such as cells. With the advent of photolithography and electron beam lithography, the trapping of objects as small as 10 nm has been enabled. The next step will be to use the electrically contacted nanowires and nanotubes themselves as the electrodes in the next generation of nanodielectrophoresis. These nanoelectrodes, perhaps themselves manipulated and interconnected with microelectrodes, will have even larger electric field gradients and will be able to manipulate 1-nm-sized objects. This is one possible route to molecular electronics. Furthermore, this will provide a new, economical, easy to handle, and direct link to the nanometer world, which could lead to many new discoveries and a truly new technology: nanotechnology.

GLOSSARY

Carbon nanotube A nanometer-scale tube of carbon atoms, which can be either metallic or semiconducting, depending on the chirality.

DEP field flow fractionation The separation of objects according to their dielectric properties.

Dielectrophoresis The force acting on a polarizable object (neutral or charged) due to an ac or dc electric field gradient.

Nanobiotechnology The control of biological processes at the nanometer length scale.

Nanowires Narrow-diameter metallic or semiconducting wires whose dimensions (typically less than 10 nm) cannot be realized by lithography alone.

Traveling wave dielectrophoresis The transport through space in three dimensions of polarizable objects due to a traveling wave electric field.

ACKNOWLEDGMENTS

Some of the experimental work presented here was performed by Sunan Liu and Lifeng Zheng. We thank J. Brody and Noo Lee Jeon for experimental assistance with the work, and Marc Madou and Shengdong Li for interesting discussions.

REFERENCES

1. H. A. Pohl, *J. Appl. Phys.* 22, 869 (1951).
2. H. A. Pohl, "Dielectrophoresis." Cambridge University Press, Cambridge, UK, 1978.
3. R. Pethig, "Dielectric and Electronic Properties of Biological Materials." Wiley, Great Britain, 1979.
4. E. H. Grant, R. J. Sheppard, and G. P. South, "Dielectric Behavior of Biological Molecules in Solution." Oxford University Press, Oxford, UK, 1978.
5. R. Pethig and G. H. Markx, *Trends Biotechnol*. 15, 426 (1997).
6. R. Pethig, *Crit. Rev. Biotechnol.* 16, 331 (1996).
7. U. Zimmermann and G. A. Neil, "Electromanipulation of Cells." CRC Press, Boca Raton, FL, 1996.
8. G. Fuhr, U. Zimmermann, and S. G. Shirley, in "Electromanipulations of Cells" (U. Zimmerman and G. A. Neil, Eds.). CRC Press, Boca Raton, FL, 1996.
9. M. J. Madou, "Fundamentals of Microfabrication," 2nd ed. CRC Press, Boca Raton, FL, 2002.
10. M. P. Hughes, *Nanotechnology* 11, 124 (2000).
11. T. B. Jones, "Electromechanics of Particles." Cambridge University Press, Cambridge, UK, 1995.
12. W. M. Arnold, H. P. Schwan, and U. Zimmerman, *J. Phys. Chem.* 91, 5093 (1987).
13. C. Li, D. Holmes, and H. Morgan, *Electrophoresis* 22, 3893 (2001).
14. M. P. Hughes and N. G. Green, *J. Colloid. Interf. Sci.* 250, 266 (2002).
15. N. F. Ramsey, "Molecular Beams." Oxford University Press, London, 1956.
16. X. Wang, X. B. Wang, F. F. Becker, and P. R. C. Gascoyne, *J. Phys. D* 29, 1649 (1996).
17. D. S. Clague and E. K. Wheeler, *Phys. Rev. E* 64, 026605 (2001).
18. Y. Huang and R. Pethig, *Measurement Science and Technology* 2, 1142 (1991).
19. X. B. Wang, Y. Huang, X. Wang, F. F. Becker, and P. R. C. Gascoyne, *Biophys. J*. 72, 1887 (1997).
20. G. Fuhr, W. M. Arnold, R. Hagedorn, T. Müller, W. Benecke, B. Wagner, and U. Zimmermann, *Biochim. Biophys. Acta* 1108, 215 (1992).
21. T. Schnelle, R. Hagedorn, G. Fuhr, S. Fiedler, and T. Müller, *Biochim. Biophys. Acta* 1157, 127 (1993).
22. L. Zheng, P. J. Burke, and J. P. Brody, unpublished.
23. T. Müller, A. M. Gerardino, T. Schnelle, S. G. Shirley, G. Fuhr, G. Degasperis, R. Leoni, and F. Bordoni, *Nuovo Cimento* 17, 425 (1995).
24. T. Müller, A. Gerardion, T. Schnelle, S. G. Shirley, F. Bordoni, G. De Gasperis, R. Leoni, and G. Fuhr, *J. Phys. D* 29, 340 (1996).
25. M. G. Green and H. Morgan, *J. Phys. D* 30, L41 (1997).
26. M. P. Hughes and H. Morgan, *J. Phys. D* 31, 2205 (1998).
27. N. G. Green and H. Morgan, *J. Phys. D* 31, L25 (1998).
28. M. P. Hughes and H. Morgan, *Anal. Chem.* 71, 3441 (1999).
29. M. P. Hughes, H. Morgan, and M. F. Flynn, *J. Colloid. Interf. Sci.* 220, 454 (1999).
30. M. P. Hughes, *J. Colloid. Interf. Sci.* 250, 291 (2002).
31. N. G. Green and H. Morgan, *J. Phys. B* 103, 41 (1999).
32. P. J. Burke, unpublished.
33. W. M. Arnold and U. Zimmermann, *J. Electrostat.* 21, 151 (1988).
34. R. Hagedorn, G. Fuhr, T. Müller, and J. Gimsa, *Electrophoresis* 13, 49 (1992).
35. G. Fuhr, S. Fiedler, T. Müller, T. Schnelle, H. Glasser, T. Lisec, and B. Wagner, *Sensor. Actuator.* 41–42, 230 (1994).
36. X. B. Wang, R. Pethig, and T. B. Jones, *J. Phys. D* 25, 905 (1992).
37. X. B. Wang, Y. Huand, R. Hölzel, J. P. H. Burt, and R. Pethig, *J. Phys. D* 26, 312 (1993).
38. M. P. Hughes, R. Pethig, and X. B. Wang, *J. Phys. D* 28, 474 (1995).
39. X. B. Wang, Y. Huang, F. F. Becker, and P. R. C. Gascoyne, *J. Phys. D* 27, 1571 (1994).
40. X. B. Wang, M. P. Hughes, Y. Huang, F. F. Becker, and P. R. C. Gascoyne, *Biochim. Biophys. Acta* 1243, 185 (1995).
41. A. Ashkin, *Phys. Rev. Lett.* 40, 729 (1978).
42. P. W. Smith, A. Ashkin, and W. J. Tomlinson, *Opt. Lett.* 6, 284 (1981).
43. A. Ashkin, J. M. Dziedzic, and P. M. Smith, *Opt. Lett.* 7, 276 (1982).
44. A. Ashkin, J. M. Dziedzic, J. E. Bjorkholm, and S. Chu, *Opt. Lett.* 11, 288 (1986).
45. A. Ashkin, *Biophys. J.* 61, 569 (1992).
46. K. Svoboda and S. M. Block, *Annu. Rev. Biophys. Biom.* 23, 247 (1994).
47. G. Fuhr, H. Glasser, T. Müller, and T. Schnelle, *Biochim. Biophys. Acta* 1201, 353 (1994).
48. T. Yamamoto, O. Kurosawa, H. Kabata, N. Shimamoto, and M. Washizu, *IEEE Trans. Indust. Appl.* 36, 1010 (2000).
49. J. S. Batchelder, U.S. Patent 4, 390, 403, 1983.
50. J. S. Batchelder, *Rev. Sci. Instrum.* 54, 300 (1983).
51. S. Masuda, M. Washizu, and Iwadare, *IEEE Trans. Indust. Appl.* IA-23, 474 (1987).
52. S. Masuda, M. Washizu, and I. Kawabata, *IEEE Trans. Indust. Appl.* 24, 217 (1988).
53. S. Masuda, M. Washizu, and T. Nanba, *IEEE Trans. Indust. Appl.* 25, 732 (1989).
54. M. Washizu, T. Nanba, and S. Masuda, *IEEE Trans. Indust. Appl.* 26, 352 (1990).
55. S. Liu, P. J. Burke, and J. P. Brody, unpublished.
56. H. A. Pohl and I. Hawk, *Science* 152, 647 (1966).
57. I. P. Ting, K. Jolley, C. A. Beasley, and H. A. Pohl, *Biochim. Biophys. Acta* 234, 324 (1971).
58. P. Marszalek, J. J. Jielinski, and M. Fikus, *Biochemistry and Bioenergetics* 22, 289 (1989).
59. R. Pethig, Y. Huang, X.-B. Wang, and J. P. H. Burt, *J. Phys. D* 25, 881 (1992).
60. Y. Huang, R. Hölzel, R. Pethig, and X. B. Wang, *Phys. Med. Biol.* 37, 1499 (1992).
61. G. H. Markx, M. S. Talary, and R. Pethig, *J. Biotechnol.* 32, 29 (1994).
62. X. B. Wang, Y. Huang, J. P. H. Burt, G. H. Markx, and R. Pethig, *J. Phys. D* 26, 1278 (1993).
63. G. H. Markx, Y. Huang, X. F. Zhou, and R. Pethig, *Microbiology-UK* 140, 585 (1994).
64. G. H. Markx, P. A. Dyda, and R. Pethig, *J. Biotechnol.* 51, 175 (1996).
65. F. F. Becker, X. B. Wang, Y. Huang, R. Pethig, J. Vykoukal, and P. R. C. Gascoyne, *J. Phys. D* 27, 2659 (1994).
66. F. Becker, X. B. Wang, Y. Huang, R. Pethig, J. Vykoukal, and P. R. C. Gascoyne, *Proc. Natl. Acad. Sci.* 92, 860 (1995).
67. M. Stephens, M. S. Talary, R. Pethig, A. K. Burnett, and K. I. Mills, *Bone Marrow Transpl.* 18, 777 (1996).
68. G. Fuhr, R. Hagedorn, T. Müller, W. Benecke, B. Wagner, and J. Gimsa, *Stud. Biophys.* 140, 79 (1991).
69. M. S. Talary, J. P. H. Burt, J. A. Tame, and R. Pethig, *J. Phys. D* 29, 2198 (1996).
70. N. G. Green, M. P. Hughes, W. Monaghan, and H. Morgan, *Microelectron. Eng.* 35, 421 (1997).
71. G. H. Markx and R. Pethig, *Biotech. Bioengineering* 45, 337 (1995).

72. K. L. Chan, H. Morgan, E. Morgan, I. T. Cameron, and M. R. Thomas, *Biochim. Biophys. Acta* 1500, 313 (2000).
73. X. B. Wang, J. Yang, Y. Huang, J. Vykoukal, F. Becker, and P. R. C. Gascoyne, *Anal. Chem.* 72, 832 (2000).
74. J. A. R. Price, J. P. H. Burt, and R. Pethig, *Biochim. Biophys. Acta* 964, 221 (1988).
75. J. Cheng, E. L. Sheldon, L. Wu, M. J. Heller, and J. P. O'Connell, *Anal. Chem.* 70, 2321 (1998).
76. J. Voldman, M. L. Gray, M. Toner, and M. A. Schmidt, *Anal. Chem.* 74, 3984 (2002).
77. S. Archer, T. Li, A. T. Evans, S. T. Britland, and H. Morgan, *Biochem. Biophys. Res. Co.* 257, 687 (1999).
78. J. Cheng, E. L. Sheldon, L. Wu, A. Uribe, L. O. Gerrue, J. Carrino, M. J. Heller, and J. P. O'Connell, *Nat. Biotechnol.* 16, 541 (1998).
79. Y. Huang, K. L. Ewalt, M. Tirado, R. Haigis, A. Foster, D. Ackley, M. J. Heller, J. P. O'Connell, and M. Krihak, *Anal. Chem.* 73, 1549 (2001).
80. Y. Huang, S. Joo, M. Duhon, M. Heller, B. Wallace, and X. Xu, *Anal. Chem.* 74, 3362 (2002).
81. J. M. Yang, J. Bell, Y. Huang, M. Tirado, D. Thomas, A. H. Forster, R. W. Haigis, P. D. Swanson, R. B. Wallace, B. Martinsons, and M. Krihak, *Biosensors and Bioelectronics* 17, 605 (2002).
82. J. C. Giddings, *Sep. Sci. Technol.* 19, 831 (1984).
83. J. M. Davis and J. C. Giddings, *Sep. Sci. Technol.* 21, 969 (1986).
84. M. Washizu, S. Suzuki, O. Kurosawa, T. Nishizaka, and T. Shinohara, *IEEE Trans. Indust. Appl.* 30, 835 (1994).
85. G. H. Markx, J. Rousselet, and R. Pethig, *J. Liq. Chromatogr. R. T.* 20, 2857 (1997).
86. Y. Huang, X. B. Wang, F. F. Becker, and P. C. Gascoyne, *Biophys. J.* 73, 1118 (1997).
87. G. H. Markx, R. Pethig, and J. Rousselet, *J. Phys. D* 30, 2470 (1997).
88. J. Rousselet, G. H. Markx, and R. Pethig, *Colloids and Surfaces A* 140, 209 (1998).
89. X. B. Wang, J. Vykoukal, F. F. Becker, and P. R. C. Gascoyne, *Biophys. J.* 74, 2689 (1998).
90. Y. Huang, J. Yang, X. B. Wang, F. F. Becker, and P. R. C. Gascoyne, *J. Hematoth. Stem Cell* 8, 481 (1999).
91. P. Debye, P. P. Debye, and B. H. Eckstein, *Phys. Rev.* 94, 1412 (1954).
92. P. Debye, P. P. Debye, B. H. Eckstein, W. A. Barber, and G. J. Arquette, *J. Chem. Phys.* 22, 152 (1954).
93. A. Prock and G. McConkey, *J. Chem. Phys.* 32, 224 (1960).
94. A. Lösche and H. Hultschig, *Kolloid-Zeitschrift* 141, 177 (1955) (in German).
95. M. Eisenstadt and I. H. Scheinberg, *Science* 176, 1335 (1972).
96. M. Eisenstadt and H. Scheinberg, *Biopolymers* 12, 2491 (1973).
97. A. Bezryadin and C. Dekker, *J. Vac. Sci. Technol. B* 15, 793 (1997).
98. A. Bezryadin, C. Dekker, and G. Schmid, *Appl. Phys. Lett.* 71, 1273 (1997).
99. J. Priestley, "The History and Present State of Electricity with Original Experiments," 2nd ed. London, 1769.
100. T. C. Halsey and W. Toor, *Phys. Rev. Lett.* 65, 2820 (1990).
101. A. Bezryadin, R. M. Westervelt, and M. Tinkham, *Appl. Phys. Lett.* 74, 2699 (1999).
102. I. Amlani, A. M. Rawlett, L. A. Nagahara, and R. K. Tsui, *Appl. Phys. Lett.* 80, 2761 (2002).
103. J. Chen, W. Wang, M. A. Reed, A. M. Rawlett, D. W. Price, and J. M. Tour, *Appl. Phys. Lett.* 77, 1224 (2000).
104. K. D. Hermanson, S. O. Lumsdon, J. P. Williams, E. W. Kaler, and O. D. Velev, *Science* 294, 1082 (2001).
105. M. Washizu and O. Kurosawa, *IEEE Trans. Indust. Appl.* 26, 1165 (1990).
106. M. Washizu, O. Kurosawa, I. Arai, S. Suzuki, and N. Shimamoto, *IEEE Trans. Indust. Appl.* 31, 447 (1995).
107. H. Kabata, O. Kurosawa, I. Arai, M. Washizu, S. Margarson, R. Glass, and N. Shimamoto, *Science* 262, 1561 (1993).
108. N. Shimamoto, *J. Biol. Chem.* 274, 15293 (1999).
109. M. Ueda, H. Iwasaki, O. Kurosawa, and M. Washizu, *Jpn. J. Appl. Phys. 1* 38, 2118 (1999).
110. H. Kabata, W. Okada, and M. Washizu, *Jpn. J. Appl. Phys. 1* 39, 7164 (2000).
111. S. Suzuki, T. Yamanashi, S. Tazawa, O. Kurosawa, and M. Washizu, *IEEE Trans. Indust. Appl.* 34, 75 (1998).
112. M. Washizu, in "Automation in Biotechnology" (I. Karube, Ed.). Elsevier, New York, 1991.
113. in "Nanofabrication and Biosystems" (H. C. Hoch, L. W. Jelinski, and H. G. Craighead, Eds.), pp. 80–96. Cambridge University Press, Cambridge, UK, 1996.
114. C. L. Asbury and G. van den Engh, *Biophys. J.* 74, 1024 (1998).
115. C. L. Asbury, A. H. Diercks, and G. van den Engh, *Electrophoresis* 23, 2358 (2002).
116. M. Ueda, K. Yoshikawa, and M. Doi, *Polym. J.* 29, 1040 (1997).
117. C.-F. Chou, J. O. Tegenfeldt, O. Bakajin, S. S. Chan, E. C. Cox, N. Darnton, T. Duke, and R. H. Austin, *Biophys. J.* 83, 2170 (2002).
118. S. Tsukahara, K. Yamanaka, and H. Watarai, *Chem. Lett.* 3, 250 (2001).
119. D. Porath, A. Bezryadin, S. de Vries, and C. Dekker, *Nature* 403, 635 (2000).
120. C. Dekker and M. A. Ratner, *Phys. World* 14, 29 (2001).
121. T. Schnelle, T. Müller, S. Fiedler, S. G. Shirley, K. Ludwig, A. Herrmann, G. Fuhr, B. Wagner, and U. Zimmermann, *Naturwissenschaften* 83, 172 (1996).
122. T. Müller, S. Fiedler, T. Schnelle, K. Ludwig, H. Jung, and G. Fuhr, *Biotechnol. Tech.* 10, 221 (1996).
123. H. Morgan and N. G. Green, *J. Electrostat.* 42, 279 (1997).
124. N. G. Green, H. Morgan, and J. J. Milner, *J. Biochem. Biophys. Meth.* 35, 89 (1997).
125. M. P. Hughes, H. Morgan, F. J. Rixon, J. P. H. Burt, and R. Pethig, *Biochim. Biophys. Acta* 1425, 119 (1998).
126. M. P. Hughes, H. Morgan, and F. J. Rixon, *Eur. Biophys. J.* 30, 268 (2001).
127. M. P. Hughes, H. Morgan, and F. J. Rixon, *Biochim. Biophys. Acta* 1571, 1 (2002).
128. H. Morgan, M. P. Hughes, and N. G. Green, *Biophys. J.* 77, 516 (1999).
129. R. H. Garrett and C. M. Grisham, "Biochemistry." Saunders, Orlando, FL, 1999.
130. A. Pandey and M. Mann, *Nature* 405, 837 (2000).
131. M. Fujimori, K. Kikuchi, K. Yoshioka, and S. Kubota, *Biopolymers* 18, 2005 (1979).
132. R. Pethig and D. B. Kell, *Phys. Med. Biol.* 32, 933 (1987).
133. S. Takashima, "Electrical Properties of Biopolymers and Membranes." Adam Hilger, Bristol, England, 1989.
134. D. Pörschke, *Annu. Rev. Phys. Chem.* 36, 159 (1985).
135. A. M. Kelley, X. Michalet, and S. Weiss, *Science* 262, 1671 (2001).
136. T. Kawabata and M. Washizu, *IEEE Trans. Indust. Appl.* 37, 1625 (2001).
137. M. Washizu, M. Shikida, S. Aizawa, and H. Hotani, *IEEE Trans. Indust. Appl.* 28, 1194 (1992).
138. L. X. Benedict, S. G. Louie, and M. L. Cohen, *Phys. Rev. B* 52, 8541 (1995).
139. K. Yamamoto, S. Akita, and Y. Nakayama, *Jpn. J. Appl. Phys. 2* 31, L34 (1998).
140. F. Wakaya, T. Nagai, and K. Gamo, *Microelectron. Eng.* 63, 27 (2002).
141. X. Q. Chen, T. Saito, H. Yamada, and K. Matsushige, *Appl. Phys. Lett.* 78, 3714 (2001).
142. K. Yamamoto, S. Akita, and Y. Nakayama, *J. Phys. D* 31, L34 (1998).
143. K. Bubke, H. Grewuch, M. Hempstead, J. Hammer, and M. L. H. Green, *Appl. Phys. Lett.* 71, 1906 (1997).

144. R. Krupke, F. Hennrich, H. B. Weber, D. Beckmann, O. Hampe, and S. Malik, Contacting single bundles of carbon nanotubes with alternating electric fields, arXiv:cond-mat/0101574v1, 2002.
145. L. A. Nagahara, I. Amlani, J. Lewenstein, and R. K. Tsui, *Appl. Phys. Lett.* 80, 3826 (2002).
146. M. R. Diehl, S. N. Yaliraki, R. A. Beckman, M. Barahona, and J. R. Heath, *Angew. Chem. Int. Ed.* 41, 353 (2002).
147. H. Dai, in "Carbon Nanotubes Synthesis, Structures, Properties, and Applications" (M. S. Dresselhaus, G. Dresselhaus, and Ph. Avouris, Eds.). Topics in Applied Physics, Vol. 80. Springer, Berlin, 2001.
148. J. Kong, H. T. Soh, A. M. Cassell, C. F. Quate, and H. J. Dai, *Nature* 395, 878 (1998).
149. Y. Avigal and R. Kalish, *Appl. Phys. Lett.* 78, 2291 (2001).
150. Y. Zhang, A. Chang, J. Cao, Q. Wang, W. Kim, Y. Li, N. Morris, E. Yenilmez, J. Kong, and H. Dai, *Appl. Phys. Lett.* 79, 3155 (2001).
151. A. Ural, Y. Li, and H. Dai, *Appl. Phys. Lett.* 81, 3464 (2002).
152. B. M. I. van der Zande, G. J. M. Koper, and H. N. W. Lekkerkerker, *J. Phys. B* 103, 5754 (1999).
153. P. A. Smith, C. D. Nordquist, T. N. Jackson, T. S. Mayer, B. R. Martin, J. Mbindyo, and T. E. Mallouk, *Appl. Phys. Lett.* 77, 1399 (2000).
154. X. Duan, Y. Huand, Y. Cul, J. Wang, and C. M. Lieber, *Nature* 409, 66 (2001).
155. J. Chen, M. A. Reed, A. M. Rawlett, and J. W. Tour, *Science* 286, 1550 (1999).
156. M. A. Reed, J. Chen, A. M. Rawlett, D. W. Price, and J. M. Tour, *Appl. Phys. Lett.* 78, 3735 (2001).
157. M. A. Reed, C. Zhou, C. J. Muller, T. P. Burgin, and J. M. Tour, *Science* 278, 252 (1997).
158. R. Hagedorn, G. Fuhr, T. Müller, T. Schnelle, U. Schnakenberg, and B. Wagner, *J. Electrostat.* 33, 159 (1994).
159. M. P. Hughes, *Nanotechnology* 13, 157 (2002).
160. K. E. Drexler, "Nanosystems: Molecular Machinary, Manufacturing, and Computation." Wiley, New York, 1992.
161. R. Feynman, *Microelectromechanical Systems* 1, 60 (1992), reprinted from 1960 speech at Caltech.
162. M. Grandbois, M. Beyer, M. Rief, H. Clausen-Schaumann, and H. E. Gaub, *Science* 283, 1727 (1999).
163. N. G. Green, A. Ramos, H. Morgan, and A. Castellanos, *Electrostatics 1999, Institute of Physics Conference Series* 163, 89 (1999).
164. B. Ladoux, H. Isambert, J. Leger, and J. Viovy, *Phys. Rev. Lett.* 81, 3793 (1998).
165. A. Ramos, H. Morgan, N. G. Green, and A. Castellanos, *J. Phys. D* 31, 3338 (1998).
166. A. Ramos, H. Morgan, N. G. Green, and A. Castellanos, *J. Electrostat.* 47, 71 (1997).
167. A. Ramos, H. Morgan, N. G. Green, and A. Castellanos, *J. Colloid. Interf. Sci.* 217, 420 (1999).
168. N. G. Green, A. Ramos, and H. Morgan, *J. Phys. D* 33, 632 (2000).
169. N. G. Green, A. Ramos, A. Gonzalez, H. Morgan, and A. Castellanos, *Phys. Rev. E* 61, 4011 (2000).